

Detection and classification of faults in induction motor by means of motor current signature analysis and stray flux monitoring

Abstract. In this paper the detection and classification of faults in induction motor using motor current signature analysis and monitoring of stray flux are presented. During the research motors with static, dynamic and mixed eccentricity were measured. The results were analyzed and compared with the data obtained from the simulated motor models. The behavior of sidebands of principal slot harmonics was examined. The results are presented in the form of graphs that illustrate the effectiveness and advantage of the method for diagnosis of the motor and detection of faults in it.

Streszczenie. W artykule przedstawiono metodę detekcji i klasyfikacji defektów silników indukcyjnych na podstawie analizy prądu i strumienia rozprzószonego. Możliwe jest wykrywanie statycznych i dynamicznych ekcentryczności. Zmierzone parametry były porównywane z danymi otrzymanymi metodą symulacji. **Detekcja i klasyfikacja defektów silnika indukcyjnego na podstawie analizy prądu i strumienia rozprzószonego.**

Keywords: induction motor faults, eccentricity, stray flux monitoring, motor current signature analysis

Słowa kluczowe: silnik indukcyjny, wykrywanie defektów, analiza prądu silnika indukcyjnego

Introduction

Induction machines are characterized by the high importance for different branches of industry in the whole world. They act as crucial component for any industrial system in a wide range of power.

Advance and accurate detection of incipient faults of induction motors and their diagnosis allow to avoid harmful and destructive outcome and prevent financial losses [1].

Eccentricity fault is one of the most significant types of faults in induction [2]-[4] as well as in the synchronous machines [5]. Machine eccentricity is characterized by unequal air-gap that exists between the stator and rotor. In the case when eccentricity enlarges, unbalanced radial forces that also can be known as unbalanced magnetic pull, can cause stator to rotor rub. There exist two types of eccentricity: static air-gap eccentricity and dynamic air-gap eccentricity. In reality both static and dynamic eccentricities tend to coexist. An inherent level of static eccentricity exists even in newly manufactured machines peculiarities of manufacturing and assembly method. It can result in steady unbalanced one direction magnetic pull. During the operation, this may lead to bent rotor shaft, bearing wear and tear, etc. Moreover, this can become a reason for a certain degree of dynamic eccentricity. In the case when these effects are not detected on early stage they can lead to rotor hub, which, in turn, will cause major breakdown of the machine.

In the presented paper electrical condition monitoring using motor current signature analysis (MCSA) is chosen. MCSA utilizes spectral analysis results of the three phase stator current of induction motor to detect faults that are present in it [6]-[10]. As well as the current signal, the magnetic flux density in the air-gap and outside the motor were also examined [11]. The magnetic flux density or the stray flux of electrical machine represents the flux that is radiated by motor outside its housing. Hence it is affected by the presence of the typical faults in the machine [12]-[16].

For clear understanding of the occurrence and presence of characteristic frequencies and other peaks in the spectrums, the behavior of the magnetic flux density depending on the time, together with spatial variation in the air-gap were considered. Measured data from the real motors was compared with the previously simulated models, the analysis of this comparison is presented below.

Fault effect on frequency spectrum

The harmonic content in the spectrum of magnetic flux density may be described using analysis of the magnetic flux density in the airgap of the motor as a function of time and angle in the same time [12], [17]. Such consideration allows to see the direct dependence of the principal slot harmonics (PSH) as well as fundamental frequency and its multiples on the fundamental number of pole pairs as well as the number of stator or rotor slots.

There are two ways of analysis of the motor without any asymmetry: only rotor slots are taken into account and stator is considered as smooth, and vice versa - stator slots are taken into account and rotor is considered to be smooth.

The length of the motor airgap is

$$(1) \quad \delta(\theta) = \delta + \Delta(\theta)$$

where δ – is initial length of the airgap, Δ – is the airgap change that represents the influence of the rotor slot openings along the airgap function.

The airgap change is

$$(2) \quad \Delta(\theta) = \frac{1}{f(\theta)} - \delta$$

where $f(\theta)$ – is a periodic function whose period is the stator (rotor) slot pitch.

The decomposed into harmonics periodic function for the case of slotted rotor is

$$(3) \quad f(\theta_m, t) = a_{r0} - \sum_{\nu=1}^{\infty} a_{r\nu} \cdot \cos \nu(Q_r \theta_m - Q_r \omega_r t)$$

where Q_r – is number of rotor slots, $\nu=1,5,7,\dots$ is order of harmonics.

Calculation of value of the coefficient $a_{r\nu}$ for slotted rotor, and $a_{s\nu}$ for slotted stator is based on the Carter's method [17] and as expected,

$$(4) \quad a_{r0} \approx \frac{1}{K_{c1}\delta}, a_{s0} \approx \frac{1}{K_{c2}\delta}$$

where K_{c1} – is Carter's factor for rotor slotting, K_{c2} – is Carter's factor in the case of stator slotting.

The inverse airgap function in the form of DC component and the first harmonic for the case of slotted rotor is

$$(5) \quad \lambda(\theta_m, t) = \frac{1}{\delta} \cdot \left[\frac{1}{K_{c1}} - k_{rs} \cdot \cos(Q_r \theta_m - Q_r \omega_r t) \right]$$

where k_{rs} as well as k_{ss} according to the method proposed in [17] are

$$k_{rs} = \delta \cdot a_{r1}, k_{ss} = \delta \cdot a_{s1}.$$

Magnetic flux density in the case of rotor slotting is

$$(6) \quad B(\theta_m, t) = \mu_0 \cdot F_{mv} \cdot \cos(v \cdot p \cdot \theta_m - \omega_1 t) \times \frac{1}{\delta} \cdot \left[\frac{1}{K_{c1}} - k_{rs} \cdot \cos(Q_r \theta_m - Q_r \omega_r t) \right]$$

For the second case, when stator is slotted and the rotor is smooth, the derivation of final formula for magnetic flux density is similar, except the terms that correspond to frequency of rotation of rotor field, Carter's factor and coefficient k_s .

Magnetic flux density in the case of slotted stator is:

$$(7) \quad B(\theta_m, t) = \mu_0 \cdot F_{mv} \cdot \cos(v \cdot p \cdot \theta_m - \omega_1 t) \times \frac{1}{\delta} \cdot \left[\frac{1}{K_{c2}} - k_{ss} \cdot \cos(Q_s \theta_m) \right]$$

where Q_s - is the number of stator slots.

For the case when motor eccentricity is taken into account, stator and rotor are both considered as smooth. So the magnetic flux density formula for the motor with dynamic eccentricity is

$$(8) \quad B(\theta_m, t) = \frac{\mu_0}{\delta} \cdot (F_{mv} \cdot \cos(v \cdot p \cdot \theta_m - \omega_1 t)) - \frac{k_{ed} \cdot F_{mv}}{2} \left[\cos((vp-1)\theta_m - (\omega_1 - \omega_r)t) + \cos((vp+1)\theta_m - (\omega_1 + \omega_r)t) \right]$$

where k_{ed} - is the level of dynamic eccentricity.

And for the case of static eccentricity it is:

$$(9) \quad B(\theta_m, t) = \frac{\mu_0}{\delta} \cdot (F_{mv} \cdot \cos(v \cdot p \cdot \theta_m - \omega_1 t)) - \frac{k_{es} \cdot F_{mv}}{2} \left[\cos((vp-1)\theta_m - \omega_1 t) + \cos((vp+1)\theta_m - \omega_1 t) \right]$$

where k_{es} – is the level of static eccentricity.

Motor also can be analyzed considering stator slotting together with the rotor slotting, that can be found in [17].

The relation between the fault and magnetic flux density and the relation between the fault and current is similar, but it is not the same. Some of the frequencies that are present in the magnetic flux density spectrum are the same as the frequencies that can be found in the current. All of these magnetic flux density frequencies are present in the airgap of the motor, but not all of them can induce voltage to the stator winding. That is why there are difference in the frequency content of current and magnetic flux density spectrums. Unfortunately the measurement of magnetic flux density in the airgap is more difficult to implement. For the consideration of current harmonic content there exist two methods of detection of air-gap eccentricity. In most cases it may be detected with the help of certain high frequency components in the stator line current. The first method allows to monitor behavior of the current at the sidebands of the slot frequencies. The sideband frequencies associated with an eccentricity are [7]

$$(10) \quad f_{slot+ecc} = f_s \left[(kQ_r \pm n_d) \left(\frac{1-s}{p} \right) \pm n_\omega \right]$$

where $n_d = 0$ in case of static eccentricity, and $n_d = 1, 2, 3, \dots$ in case of dynamic eccentricity (n_d is known as eccentricity order), f_s is the fundamental supply frequency, Q_r is the number of rotor slots, s is the slip, p is the number of pole pairs, k is any integer, and n_ω is the order of stator time harmonics that are present in the power supply driving the motor ($n_\omega = 1, 3, 5, \dots$).

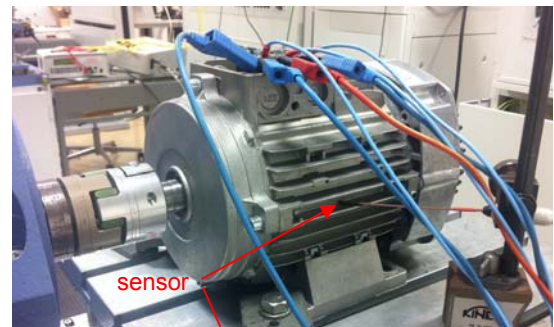
The second method is based on the monitoring of the behavior of the current at the sidebands of the supply frequency and its odd multiples. These frequencies of interest are given by

$$(11) \quad f_{ecc} = k_1 \cdot f_s \pm m \cdot f_s \cdot \left(\frac{1-s}{p} \right)$$

where m – is any integer.

Simulation and experimental results

a)



b)

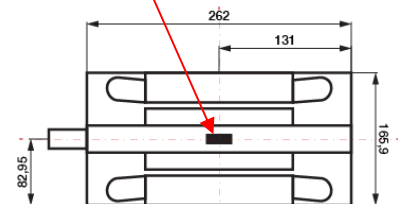


Fig. 1. Experimental installation (a) and its diagram (b) with the position of sensor

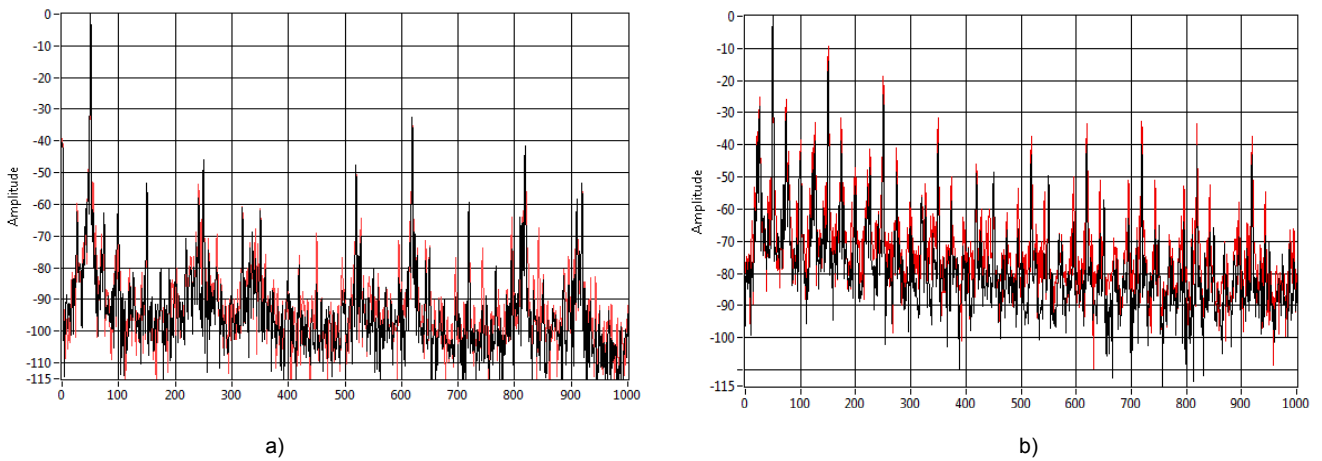


Fig. 2. Measured spectrums of current (a) and magnetic flux density (b) of the healthy motor (black) compared to the motor with dynamic eccentricity (red)

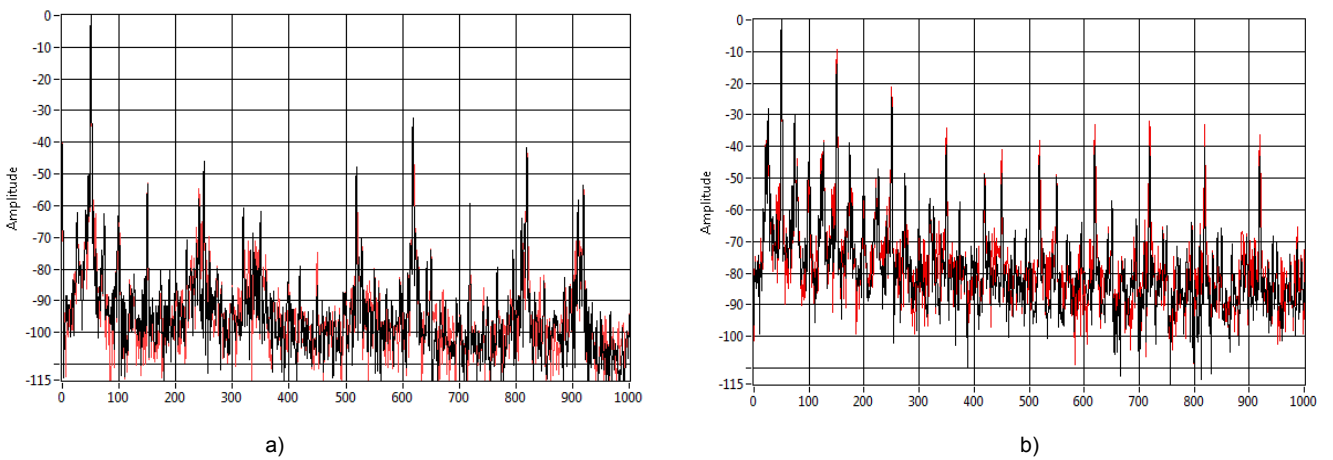


Fig. 3. Measured spectrums of current (a) and magnetic flux density (b) of the healthy motor (black) compared to the motor with static eccentricity (red)

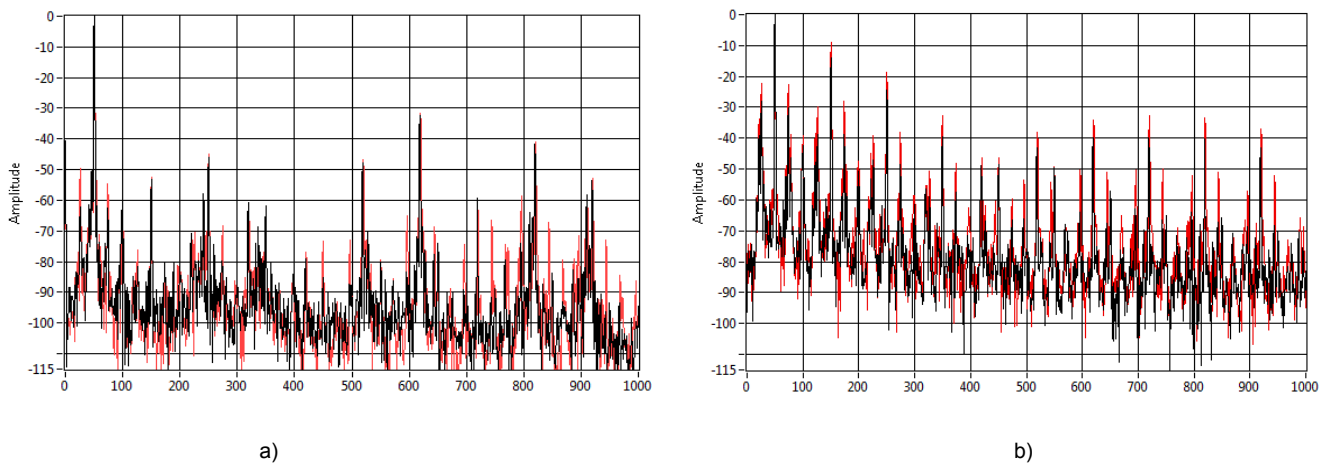


Fig. 4. Measured spectrums of current (a) and magnetic flux density (b) of the healthy motor (black) compared to the motor with mixed eccentricity (red)

The current of motor as well as its stray flux were monitored and analyzed using the experimental installation with F.W. Bell 7030 Gauss/Teslameter and the magnetic flux sensor [13], [18]. In the present experimental installation the Hall probe was used as a sensor, but there are also the other types of sensors that can be used in similar measurements [19]. Measurement results were processed using the LabVIEW System Design Software.

There were implemented simulation models of a real motor that were considered and analyzed [20]. After that the measurements of a real motor with faults were carried out.

The simulated models of induction machine were prepared for four cases - one model of healthy motor and three models with eccentricities: pure static, pure dynamic and mixed eccentricities. The modelling of these effects allows to investigate its impact on the occurrence of characteristic frequencies and slot harmonics in current spectrums and spectrums of magnetic flux.

The simulation was carried out using finite element method based on the characteristics of a real induction motor. Time step used for all simulations is 0.1 ms.

The real motor is three-phase, 4-pole, 400 V, 50 Hz, 1.1 kW squirrel-cage induction motor, that have 36 stator and 28 rotor slots. Modeling and FFT computation were carried out with the help of ANSYS Maxwell and MatLab software. All four motors have been simulated with operating speed 1440 rpm. This speed implies a slip $s = 0.04$.

There were measured motors with static, dynamic and mixed eccentricities, as well as the healthy one. Measurements were carried out for four types of loads: no-load, half-load, full load and overload.

The results obtained from the full loaded motor are considered and compared with the simulated data. Results of measurements are presented on Fig.2, Fig.3 and Fig.4 where the normalized spectrums of current and magnetic flux density of the healthy motor are compared to the motors having dynamic, static and mixed eccentricity respectively.

It is clearly seen that the current spectrums of motor with pure dynamic (Fig.2(a)) and pure static (Fig.3(a))

eccentricities are almost the same as the spectrum of healthy motor. But considering the magnetic flux density spectrum on Fig. 2(b) the presence of dynamic eccentricity is clearly visible. Hence, for the diagnosis of presence of the dynamic eccentricity fault in the motor it is better to monitor the behavior of magnetic flux density spectrum.

The value of the second principal slot harmonic should be related to static eccentricity. But in the case of this measurement it is not so. This can be concluded from the current spectrums, because the second principal slot harmonic has higher amplitude in the current spectrum of the healthy motor. But if we consider the spectrum of magnetic flux density, the rise of the amplitude of the 2nd principal slot harmonic in the motor with static eccentricity for 10 dB is clearly seen. For the other characteristic frequencies the amplitudes are almost the same as in the magnetic flux density spectrum of the healthy motor, which is shown on Fig. 3 (b).

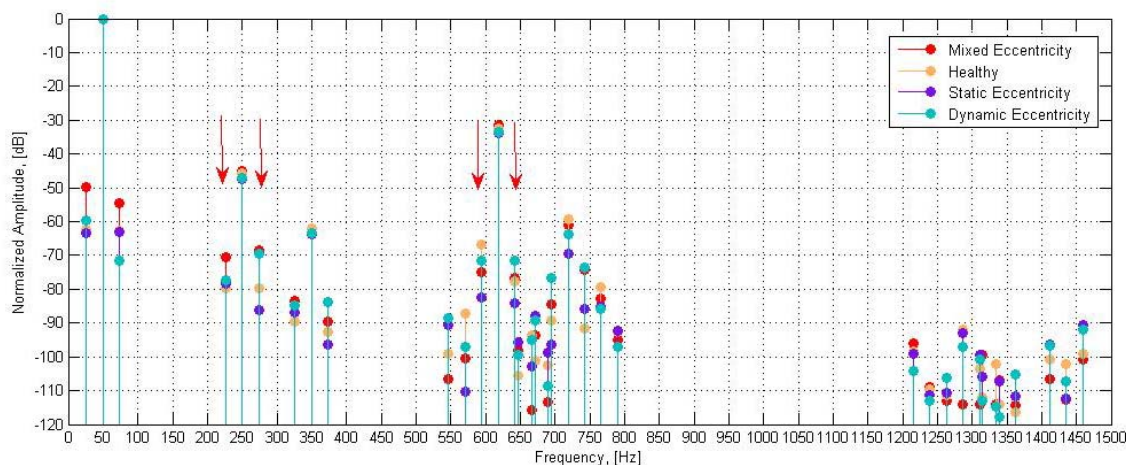


Fig. 5. Measured current amplitudes in the points of PSHs and their sidebands

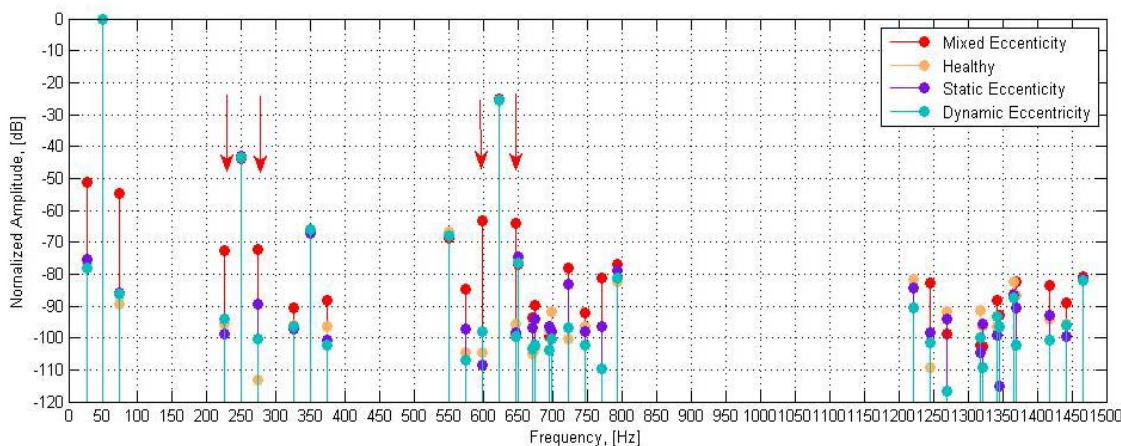


Fig.6 – Simulated current amplitudes in the points of PSHs and their sidebands

The monitoring of the current spectrum is useful for the detection of mixed eccentricity, because the characteristic frequencies are clearly visible and have higher amplitudes than in the current spectrum of healthy motor that can be clearly seen on Fig. 4(a). The spectrum of magnetic flux density for this case (Fig. 4(b)) shows clearly the presence and values of amplitudes of characteristic frequencies, so it also may be used for the detection of this type of fault.

In the obtained results there were also investigated the sidebands of the principal slot harmonics. These frequencies should be related to the dynamic eccentricity. Considering obtained results and comparing it with the simulated data it is clearly visible that the sidebands of the 1st principle slot harmonic as well as the sidebands around the 2nd one are the best for the detection of the dynamic eccentricity in the current spectrum of the motor [20]. The

same frequencies have significant amplitudes in the case of mixed eccentricity. Due to the simulated data it is clear that the sidebands of the principal slot harmonics have the highest amplitudes with the presence of mixed eccentricity. And it is clear that the amplitude of these frequencies rises with the increasing of the level of dynamic eccentricity. Relation of static eccentricity is not clear in the case of present research because it has different amplitudes (higher and lower) at different frequencies without any dependence.

The results obtained from the measurements of a real motor were compared with the simulated results. Considering current spectrum with normalized values of amplitudes it is clearly seen that the characteristic frequencies are also present in the current spectrum of simulated models. They have smaller amplitudes, but due to the absence of network noise and symmetrical construction they are clearly distinctive.

Analyzed results show that the diagnosis and monitoring of the behavior of the current and magnetic flux density spectrums are practically useful for the diagnosis of the presence of faults in the motor.

Conclusions

In this paper the effects of motor eccentricity on the generation of characteristic frequencies and principal slot harmonics in the real and simulated motors were investigated. The research was focused on the MCSA and monitoring of magnetic flux density outside the motor. There were presented derived formulas of the magnetic flux density in the airgap related to the stator and rotor slotting, as well as to motor eccentricity. The relation between the fault and magnetic flux density and the relation between the fault and current is similar, but they are not the same. Frequencies that are present in the magnetic flux density spectrum are the same as the frequencies that can be found in the current spectrum. All of these frequencies are present in the airgap of the motor, hence they can be clearly distinguished in the magnetic flux density spectrum. But not all of these frequencies can induce voltage to the stator winding due to the different number of pole pairs. That is why the frequencies that are characteristic for the eccentricity fault are not visible in the current spectrum when the pure static or pure dynamic eccentricity takes place. But they are clearly detectable in the case of the mixed eccentricity. It was demonstrated that theoretical assumptions meet the practical results, as it can be seen on the presented figures. The sidebands of the principal slot harmonics were also investigated. From the obtained results it is clear that the sidebands of the 1st principle slot harmonic as well as the sidebands around the 2nd one are the best for the detection of the dynamic eccentricity in the current spectrum of the motor. Analyzed results show that the diagnosis and monitoring of the behavior of the current and magnetic flux density spectrums are practically useful for the diagnosis of the presence of faults in the motor.

Acknowledgment

This research work has been carried out in the Centre for Research and Utilization of Renewable Energy (CVVOZE). Authors gratefully acknowledge financial support from the Ministry of Education, Youth and Sports of the Czech Republic under NPU I programme (project No. LO1210).

Authors: Ing. Ielyzaveta Ishkova, Brno University of Technology, Faculty of Electrical Engineering and Communication, Technická 3082/12, CZ-61600 Brno, E-mail: xishko00@stud.feec.vutbr.cz; Ing. Ondřej Vitek, Ph.D., Brno University of Technology, Faculty of Electrical Engineering and Communication, Technická 3082/12, CZ-61600 Brno, E-mail: viteko@feec.vutbr.cz

REFERENCES

- [1] Drif M., Cardoso A.J.M., "Airgap-Eccentricity Fault Diagnosis, in Three-Phase Induction Motors, by the Complex Apparent Power Signature Analysis," *IEEE Trans. Ind. Electron*, 55 (2008), No. 3, 1404-1410
- [2] Zagirnyak M., Mamchur D., Kalinov A., "Comparison of Induction Motor Diagnostic Methods Based on Spectra Analysis of Current and Instantaneous Power Signals," *Przeglad Elektrotechniczny*, R. 88 (2012), No. 12b, 221-224
- [3] Basak D., Tiwari A., Das S. P., "Fault Diagnosis and Condition Monitoring of Electrical Machines – A Review," *IEEE International Conference ICIT* (2006), 3061-3066
- [4] Baptista B., Mendes A., Cruz S., Cardoso A., "Temperature Distribution Inside a Three-Phase Induction Motor Running With Eccentric Airgap," *Przeglad Elektrotechniczny*, R.88 (2012), No. 1a, 96-99
- [5] Ebrahimi B.M., Faiz J., Etemadrezai M., Babaie M., "Eccentricity Fault Identification in Round Rotor Synchronous Motors Considering Load Variation," *Przeglad Elektrotechniczny*, R. 87 (2011), No. 5, 288-292
- [6] Novozhilov A., Kryukova Y., Andreyeva O., Novozhilov T., "Diagnostic System Induction Motor Rotor Eccentricity by Phase Current," *Przeglad Elektrotechniczny*, R. 90 (2014), No. 9, 157-159
- [7] Benbouzid M.E., "A Review of Induction Motors Signature Analysis as a Medium for Faults Detection," *IEEE Trans. Ind. Electron*, Vol. 47 (2000), No. 5, 984-993
- [8] Nandi S., Toliyat A., Li X., "Condition Monitoring and Fault Diagnosis of Electrical Motors – A Review," *IEEE Trans. Ind. Electron*, Vol. 20 (2005), No. 4, 719-729
- [9] Benbouzid M.E.H., Kliman G.B., "What Stator Current Processing-Based Technique to Use for Induction Motor Rotor Faults Diagnosis?" *IEEE Trans. on Energy Conversion*, Vol. 18 (2003), No. 2, 238-244
- [10] Benbouzid M. E. H., Vieira M., Theys C., "Induction Motors' Faults Detection and Localization Using Stator Current Advanced Signal Processing Techniques," *IEEE Transactions on Power Electronics*, Vol. 14 (1999), 14-22
- [11] Kindl V., Hruska K., Sobra J., Byrtus M., "Effect of Induction Machine's Load and Rotor Eccentricity on Space Harmonics in the Air Gap Magnetic Flux Density," *16th International Conference on Mechatronics – Mechatronika (ME)*, (2014), 463-468
- [12] Dorrel D.G., Thomson W.T., Roach S., "Analysis of Airgap Flux, Current, and Vibration Signals as a Function of the Combination of Static and Dynamic Airgap Eccentricity in 3-Phase Induction Motors," *IEEE Trans. Ind. Electron*, Vol. 33 (1997), No. 1, 24-34
- [13] Frosini L., Harlisca C., Szabo L., "Induction Machine Bearing Fault Detection by Means of Statistical Processing of the Stray Flux Measurement," *IEEE Trans. Ind. Electron*, Vol. 62 (2015), No.3
- [14] Negrea M. D., "Electromagnetic Flux Monitoring for Detecting Faults in Electrical Machines," Ph.D. dissertation, Dept. Elect. Commun. Eng., Helsinki Univ. Technol., Espoo, Finland, 2006.
- [15] Romary R., Pusca R., Lecoince J.P., Brudny J.F., "Electrical Machines Fault Diagnosis by Stray Flux Analysis," *IEEE Workshop on Electrical Machines Design Control and Diagnosis (WEMDCD)*, (2013), 247-256
- [16] Frosini L., Borin A., Girometta L., Venchi G., "A Novel Approach to Detect Short Circuit in Low Voltage Induction Motor by Stray Flux Measurement," *20th International Conference on Electrical Machines (ICEM)*, (2012), 1538-1544
- [17] Boldea I., Nasar S., *The Induction Machine Handbook*. Boca Raton: CRC Press, (2002)
- [18] Vitek O., Janda M., Hajek V., Bauer P., "Detection of Eccentricity and Bearing Faults Using Stray Flux Monitoring," in Proc. *IEEE SDEMPED*, Bologna, Italy, (2011), 456-461
- [19] Tumanski S., "Modern Magnetic Field Sensors – A Review," *Przeglad Elektrotechniczny*, R. 89 (2013), No. 10, 1-12
- [20] Ishkova I., Vitek O., "Diagnosis of Eccentricity and Broken Rotor Bar Related Faults of Induction Motor by Means of Motor Current Signature Analysis," *16th International Scientific Conference on Electric Power Engineering (EPE)*, Kouty nad Desnou, Czech Republic (2015), 682-686.